Tunable Diode Laser Spectroscopy of *cis*-1,2-Difluoroethylene: Rovibrational Analysis of the ν_9 and $\nu_5+\nu_{10}$ Bands and Anharmonic Force Field

Paolo Stoppa,[†] A. Pietropolli Charmet,[†] Santi Giorgianni,*[,†] Sergio Ghersetti,[†] and Alberto Gambi[‡]

Università Ca' Foscari di Venezia, DCF, D.D. 2137, I-30123 Venezia, Italy, and Università di Udine, DSTC, Via Cotonificio 108, I-33100 Udine, Italy

Received: August 8, 2002; In Final Form: November 1, 2002

cis-1,2-Difluoroethylene was synthesized, and the gas-phase infrared spectrum was investigated in the ν_9 and $\nu_5+\nu_{10}$ band region (1350−1391 cm^{-1}), at a resolution of about 0.002 cm^{-1}, employing a tunable diode laser spectrometer. These vibrations of symmetry species B_1 yield strong a-type bands. Most of the J and K structure was recorded in different subbranches and the rovibrational analysis led to the assignment of 2313 ($J \leq 64$, $K_a \leq 26$) and 1172 ($J \leq 57$, $K_a \leq 20$) transitions of the ν_9 and $\nu_5+\nu_{10}$ bands, respectively. Using Watson's A-reduction Hamiltonian in the I^r representation a set of accurate spectroscopic parameters, up to four sextic centrifugal distortion terms, was obtained for both the excited states $v_9 = 1$ and $v_5 = v_{10} = 1$. A Fermi resonance coupling constant $W = 4.2(5)$ cm^{-1} was estimated for the perturbation between the ν_9 and $\nu_5+\nu_{10}$ levels. Correlated harmonic force constants were obtained from coupled cluster CCSD(T) calculations with the cc-pVTZ basis set while the anharmonic force constants were computed at MP2 level using the same basis set. There is a good agreement with the available experimental data, in particular the equilibrium geometry compared with the experimental r_0 structure and the fundamental modes. In addition, the ab initio anharmonic force field of *cis*-1,2-difluoroethylene provided a critical assessment of the experimental spectroscopic parameters, especially in the treatments of strong Fermi interactions.

1. Introduction

Halogenated ethylenes are mainly employed as monomers for the production of synthetic resins and their accidental release in the earth's atmosphere can play a significant role as air pollutants. Emphasis should be placed not only on the direct exposure to the pollutants but also to their transformation products; the most important atmospheric transformation processes involve photolysis and chemical reactions with ozone and hydroxyl radicals.[1,2]

Infrared spectroscopy is a very powerful method for detecting trace gases and for remote sensing of atmospheric components. There is a great need for accurate spectroscopic parameters of these molecules and their determination becomes essential if you want to profit from the sensitivity of this technique.

High-resolution infrared studies of small halogenated molecules containing the reactive group >C═C< have been carried out, and results concerning selected absorptions of different fluoro-ethylenes have already been reported.[3,4] Being a strong absorber in the atmospheric window, *cis*-1,2-difluoroethylene can also contribute to the greenhouse effect and we began, some years ago, an infrared study on this molecule. The first investigation of high-resolution infrared spectra initiated with the analysis of the ν_{10} band[5] and subsequent works included TDL and FTIR studies on the ν_4 and ν_2 fundamentals,[6,7] respectively.

The low-resolution infrared spectra of *cis*-CHF═CHF were examined a long time ago[8] and band centers have been determined for all the fundamentals, some overtones and combination bands. More recently, ab initio calculations of the harmonic force field together with the vibrational frequencies have been carried out[9] and gas-phase fundamental intensities have been measured.[10] The microwave spectrum was investigated much earlier,[11] mainly in relation to the determination of the rotational constants and the dipole moment. Ground-state centrifugal distortion coefficients, obtained from ground-state combination differences, were determined up to the quartic terms from ν_{10}[5] and up to the sextic terms from ν_4, ν_{10}, and ν_2 fundamentals.[7]

The present work deals with the interpretation of the rovibrational details of ν_9 (≅1375 cm^{-1}) and $\nu_5+\nu_{10}$ (≅1365 cm^{-1}) bands of *cis*-CHF═CHF. From the whole set of the assigned transitions we were able to obtain accurate band origins and excited-state parameters for both the bands falling in the atmospheric window. A Fermi resonance coupling constant and unperturbed band origins for ν_9 and $\nu_5+\nu_{10}$ were estimated.

The recent improvement of computer facilities has enabled ab initio methods to be successfully extended to include the anharmonic part of the molecular force field. The equilibrium structure and the harmonic force constants of *cis*-CHF═CHF were determined using high-level electronic-structure calculations, CCSD(T)/cc-pVTZ. The cubic and semidiagonal quartic force constants were conveniently calculated by numerical differentiation of analytic second derivatives obtained at MP2/cc-pVTZ level of theory and used to estimate anharmonic contributions to the fundamental vibrational wavenumbers as well as to assess and assist the deperturbation of Fermi resonances.

* To whom correspondence should be addressed. E-mail: giorgian@unive.it.
[†] Università Ca' Foscari di Venezia.
[‡] Università di Udine.

10.1021/jp0218488 CCC: $25.00 © 2003 American Chemical Society
Published on Web 01/01/2003

TABLE 1: Frequencies (cm^{-1}) of *cis*-1,2-Difluoroethylene Fundamentals[a]

symmetry species	mode	wavenumber	approximate description
A_1	ν_1	3122	C−H sym. stretch
A_1	ν_2	1718.8389[b]	C=C stretch
A_1	ν_3	1263	C−H sym. in-plane wag
A_1	ν_4	1016.0179[c]	C−F sym. stretch
A_1	ν_5	235.9[d]	C=C−F sym. bend
A_2	ν_6	839	C−H asym. out-of-plane wag
A_2	ν_7	495	C=C torsion
B_1	ν_8	3136	C−H asym. stretch
B_1	ν_9	1375.0653[d]	C−H asym. in-plane wag
B_1	ν_{10}	1131.1742[e]	C−F asym. stretch
B_1	ν_{11}	769	C=C−F asym. bend
B_2	ν_{12}	756	C−H sym. out-of-plane wag

[a] From ref 8. [b] From ref 7. [c] From ref 6. [d] This work. [e] From ref 5.

2. Experimental Details

The synthesis of *cis*-1,2-difluoroethylene was obtained from 1,2-difluorotetrachloroethane according to the procedure reported in a previous work.[5] The mixture of the *cis*- and *trans*-CHF=CHF isomers was separated by fractional distillation under vacuum. The purity of the *cis*-CHF=CHF, tested by gas chromatography, was 98.5%.

The spectra were recorded in the region 1350−1391 cm^{-1}, at a resolution of about 0.002 cm^{-1}, employing the tunable diode laser spectrometer available in our laboratory. The measurements were carried out at a pressure of about 1.5 mbar using a 49 cm path cell cooled at 240 K in order to reduce hot band contributions. The instrument is interfaced to a PC that provides data acquisition, storage, and conversion into transmittance of the spectra. Absolute calibration of the spectra was based on the wavenumbers of selected SO_2 transitions measured on an FTIR spectrometer against H_2O lines.[12] The relative calibration was based on interference patterns from a 2.59 cm germanium étalon (free spectral range ≅0.0475 cm^{-1}). The absolute wavenumber accuracy of the measurements is estimated to be usually better than 0.002 cm^{-1}.

3. Results and Discussion

cis-1,2-Difluoroethylene is a planar near prolate asymmetric top molecule ($\kappa = -0.841$) of C_{2v} symmetry giving rise to 12 fundamentals (symmetry species: $5A_1$, $2A_2$, $4B_1$, and B_2). The molecular geometry together with the symmetry information and the statistical weights of the rotational levels have already been reported.[5] For completeness, the observed frequencies and an approximate description of the fundamentals are summarized in Table 1, which also reports the accurate values of band origins available from high-resolution investigations.

The spectrum analyzed covers the region 1350−1391 cm^{-1} of the ν_9 and $\nu_5+\nu_{10}$ bands whose low resolution (0.25 cm^{-1}) survey spectrum is illustrated in Figure 1. The two vibrations of symmetry species B_1 give rise to **a**-type bands showing strong Q branches at 1375.1 (ν_9) and 1365.4 cm^{-1} ($\nu_5+\nu_{10}$), and defined P and R branches. An interesting observation concerns the high-frequency side of the Q branch of the ν_9 fundamental, where weaker features at 1375.7 and 1376.8 cm^{-1} very likely coming from the hot bands $\nu_9+\nu_5-\nu_5$ and $\nu_9+2\nu_5-2\nu_5$, respectively, are also present. The high-resolution details show strong **a**-type transitions which are governed by the selection rules ($\Delta J = 0, \pm1$, $\Delta K_a = 0$, $\Delta K_c = \pm1$) and produce different even ($K_a'' + K_c'' = J''$) and odd ($K_a'' + K_c'' = J'' + 1$) subbands.

3.1. Description of the Spectrum and Analysis. The Q branch in both bands does not appear easy to analyze since the K_a structure, degrading to lower (ν_9) and higher ($\nu_5+\nu_{10}$) wavenumbers, is very dense and the subbranches $^eQ(0,1)$ and $^oQ(0,-1)$ are mostly overlapped. We thus started the investigation with the identification of the more prominent features in the P and R subbranches and began the assignments for transitions with $K_a \geq 8$ by resorting to ground-state combination differences.

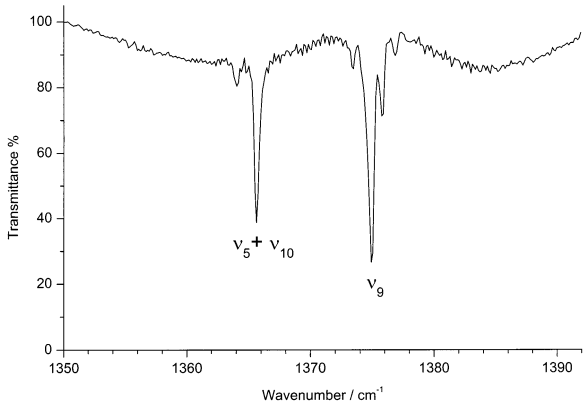

Figure 1. Survey spectrum at low resolution (0.25 cm^{-1}) of the ν_9 and $\nu_5+\nu_{10}$ bands of *cis*-CHF=CHF (room temperature, $P \cong 6$ mbar, 16 cm cell).

For medium J values, the observed details resemble the characteristics found in a parallel band of a symmetric top and within each group the assignments of the resolved lines reveal a certain degree of regularity, with consecutive unsplit features being separated by about $[(A' - A'') - (\bar{B}' - \bar{B}'')](2K + 1)$ where $\bar{B} = (B + C)/2$. As an example, a portion of the ν_9 R branch near 1380.6 cm^{-1} showing the fine structure of the ^QR_K-(14,15) manifolds is illustrated in Figure 2. The effect of the asymmetry splitting, evident for $K_a \leq 5$, gives rise to an irregular numbering of the lines with the even component located at the side of higher wavenumbers. Similar behavior is also noted in the $\nu_5+\nu_{10}$ band by looking at the spectral section near 1359.7 cm^{-1} depicted in Figure 3, where the fine structure of the ^QP_K-(16) manifold is indicated. In contrast to what was observed in the ν_9 R branch, here the split lines with the even component are located at the lower wavenumber side. For increasing J values, the features belonging to a given cluster overlap to a great extent with those of the neighboring manifolds producing an increasingly dense spectrum where the fine structure becomes more difficult to identify. In addition, because of a larger asymmetry splitting, the transitions with low K_a values give rise to spreading lines without exhibiting any regular pattern.

In carrying on the investigation with the assignments of the fine structure of groups with high J values and low K_a values we identified peculiarities generally noted in the spectra of planar molecules. In the P and R branches we observed distinct bandheads separated by about $2C = 0.31$ cm^{-1} and consisting

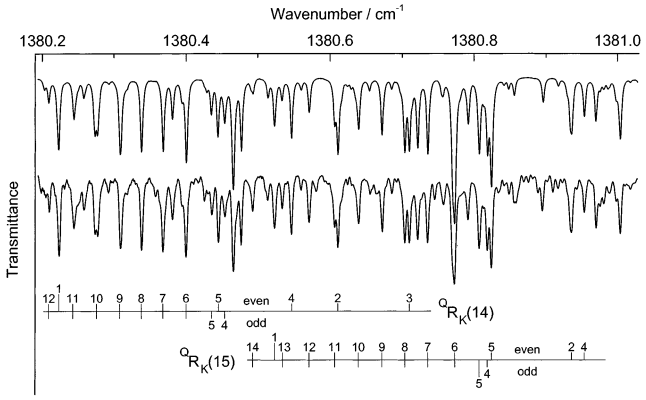

Figure 2. Portion of the R-branch spectrum of *cis*-CHF=CHF ν_9 band near 1380.6 cm^{-1} showing the K_a structure of the $^{Q}R_K(14,15)$ groups; asymmetry splitting for $K_a \leq 5$ is observed. Upper trace: simulated spectrum. Lower trace: observed spectrum ($T = 240$ K, $P \cong 1.5$ mbar, 49 cm cell). The even and odd label corresponds to ($K_a'' + K_c'' = J''$) and ($K_a'' + K_c'' = J'' + 1$), respectively.

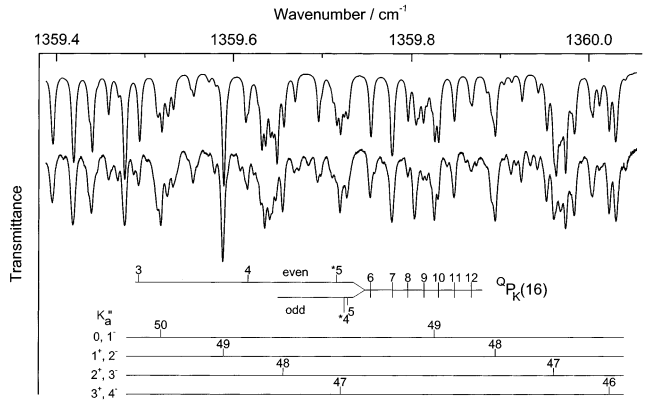

Figure 3. Details of the *cis*-CHF=CHF spectrum near 1359.7 cm^{-1} showing the line sequences in the $^{Q}P_K(16)$ group of $\nu_5+\nu_{10}$ band; lines marked by * refer to the calculated ones. Features from degenerate levels with different K_a^+ and $(K_a+1)^-$ in the $^{Q}P_K(J=50,49)$ bandheads of ν_9 band are also evident. Upper trace: simulated spectrum. Lower trace: observed spectrum ($T = 240$ K, $P \cong 1.5$ mbar, 49 cm cell). The even and odd label corresponds to ($K_a'' + K_c'' = J''$) and ($K_a'' + K_c'' = J'' + 1$), respectively.

of a series of transitions characterized by $\Delta J = 1$, $\Delta K_a = 1$, and $\Delta K_c = -2$ between successive lines each involving the almost degenerate levels with K_a^+ and $(K_a + 1)^-$ where the + and − upper signs indicate the even and odd components, respectively; this is produced by the approximation that a prolate asymmetric rotor tends to behave like an oblate symmetric rotor at low values of K_a and high values of J. A specimen spectrum can be recognized in Figure 3, where the resolved J lines in the $^{Q}P_K(J=50,49)$ bandheads of ν_9 are also indicated. As can be observed, the spectrum reproduced exhibits different transitions belonging to the ν_9 and $\nu_5+\nu_{10}$ bands; good agreement between the observed and calculated characteristics confirms the reliability of the parameters obtained in the present investigation.

Once the molecular constants were determined from the assignments of the P and R branches it was possible to identify the resolved details of the $^{Q}Q_K$ subbranches, from which we gained useful information mainly for the analysis of the ν_9 fundamental. This band center is characterized by $^{Q}Q_K$ subbranches consisting of groups of lines that begin to show resolved structure as one moves away from the origin toward lower wavenumbers. Within each cluster the resolved J components progress from the most intense line ($J = K_a$) toward higher wavenumbers until they blend into the neighboring block.

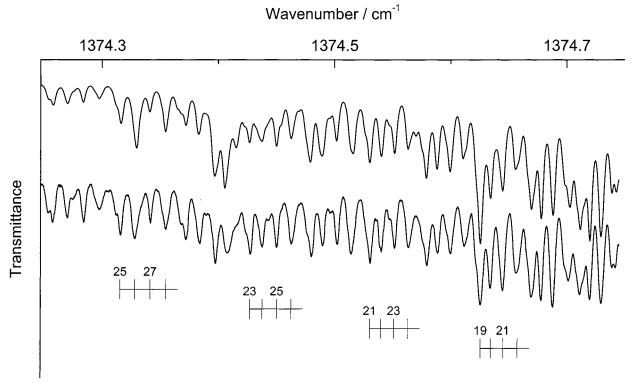

Figure 4. Details of the Q-branch spectrum of the *cis*-CHF=CHF ν_9 band showing the resolved J structure of the $^{Q}Q_K(J)$ manifolds with $K_a = 19$, 21, 23, and 25. Upper trace: simulated spectrum. Lower trace: observed spectrum ($T = 240$ K, $P \cong 1.5$ mbar, 49 cm cell).

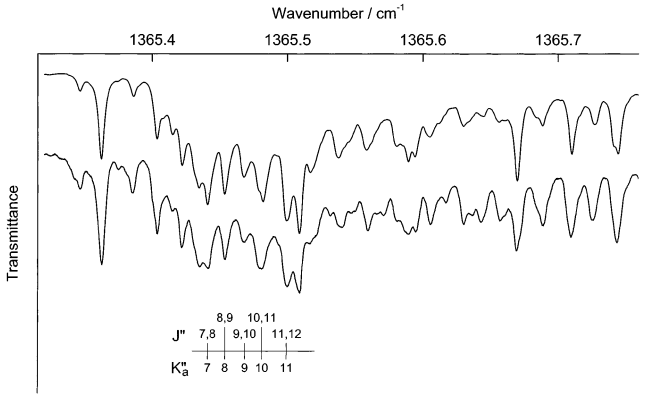

Figure 5. A section of the Q-branch spectrum of *cis*-CHF=CHF $\nu_5+\nu_{10}$ band near 1365.5 cm^{-1}. The assignment of the overcrowded transitions $^{Q}Q_7(7,8)$, $^{Q}Q_8(8,9)$, ..., $^{Q}Q_{11}(11,12)$ is illustrated. Upper trace: simulated spectrum. Lower trace: observed spectrum ($T = 240$ K, P ≅ 1.5 mbar, 49 cm cell).

A portion of the Q-branch spectrum of the ν_9 band near 1374.5 cm^{-1} containing the $^{Q}Q_{19-25}(J)$ clusters is depicted in Figure 4, where the J assignments for several manifolds are presented. The structure appears to be more difficult to identify in the Q branch of the $\nu_5+\nu_{10}$ combination band, which appears more compressed as illustrated by the spectral region near 1365.5 cm^{-1}, depicted in Figure 5. Although the number of transitions which could be assigned in this branch is very limited, nevertheless the synthetic spectrum matches very well with the experimental one.

3.2. Data analysis and Fitting Procedure. The ground and excited rotational energy levels were computed using Watson's A-reduction Hamiltonian up to the sixth order in the I^r representation,

$$\frac{\mathbf{H}}{hc} = \frac{1}{2}(B+C)\mathbf{P}^2 + \left[A - \frac{1}{2}(B+C)\right]\mathbf{P}_a^2 - \Delta_J\mathbf{P}^4 - \Delta_{JK}\mathbf{P}^2\mathbf{P}_a^2 - \Delta_K\mathbf{P}_a^4 + \Phi_J\mathbf{P}^6 + \Phi_{JK}\mathbf{P}^4\mathbf{P}_a^2 + \Phi_{KJ}\mathbf{P}^2\mathbf{P}_a^4 + \Phi_K\mathbf{P}_a^6 + \left[\frac{1}{2}(B-C) - 2\delta_J\mathbf{P}^2 + 2\phi_J\mathbf{P}^4\right](\mathbf{P}_b^2 - \mathbf{P}_c^2) + [(-\delta_K\mathbf{P}_a^2 + \phi_{JK}\mathbf{P}^2\mathbf{P}_a^2 + \phi_K\mathbf{P}_a^4), \quad (\mathbf{P}_b^2 - \mathbf{P}_c^2)]_+$$

where $\mathbf{P}$ is the operator for the reduced angular momentum and $\mathbf{P}_a$, $\mathbf{P}_b$, and $\mathbf{P}_c$ are its components along the principal inertial axes in the molecular-fixed coordinate system and $[\ ]_+$ is the anticommutator.

The assignment of the transitions of the ν_9 and $\nu_5+\nu_{10}$ bands started from $^{Q}P_K(J)$ and $^{Q}R_K(J)$ manifolds characterized by

TABLE 2: Molecular Constants (cm^{-1}) for the ν_9 and $\nu_5+\nu_{10}$ Bands of cis-CHF=CHF[a]

	ground State[b]	$v_9 = 1$	$v_5 = v_{10} = 1$
ν_0		1375.06531(5)	1365.4012(1)
A	0.70393454	0.7026740(9)	0.704737(2)
B	0.19780931	0.1982842(3)	0.1981214(7)
C	0.15418069	0.1541558(2)	0.1539601(4)
$\Delta_J \times 10^6$	0.24516	0.2465(1)	0.2419(4)
$\Delta_{JK} \times 10^5$	−0.16067	−0.16116(8)	−0.1599(2)
$\Delta_K \times 10^5$	0.48831	0.4811(4)	0.494(2)
$\delta_J \times 10^7$	0.7299	0.7388(9)	0.720(3)
$\delta_K \times 10^6$	0.4373	0.4369(8)	0.458(2)
$\Phi_J \times 10^{12}$	0.560	0.55(3)	0.8(1)
$\Phi_{KJ} \times 10^{10}$	−0.487	−0.55(2)	−0.34(8)
$\Phi_K \times 10^9$	0.1375	0.156(5)	0.8(4)
$\phi_J \times 10^{12}$	0.228	0.24(2)	0.24(9)
no. of data		2313	1172
$\sigma \times 10^3$		0.647	0.771

[a] Quoted uncertainties are one standard deviation in units of the last significant digit. [b] From ref 7.

medium J and K_a quantum numbers. Following estimation of satisfactory band origin from the high- and low-wavenumber edge of the Q branch for the ν_9 and $\nu_5+\nu_{10}$ bands, respectively, the least-squares routine was carried out keeping the ground-state constants fixed to the values of ref 7 and refining the upper state parameters together with the band origin. The refining procedure was iteratively applied until the analysis was completed with the identification of resolved ^QQ_K details in the very dense Q branches. The assignment of the transitions was not straightforward because the spectrum is quite complex due to the high density of lines and the weak features coming from "hot bands". The whole analysis in the P, Q, and R branches led to the identification of 2313 ($J \leq 64$, $K_a \leq 26$) and 1172 ($J \leq 57$, $K_a \leq 20$) transitions of many subbands belonging to the ν_9 and $\nu_5+\nu_{10}$ bands, respectively. Unit weight was given to lines appearing as simple transitions, while blended or scarcely resolved features were weighted with a factor of 0.1; badly overlapped characteristics were not considered and excluded from the fit. The parameters obtained, given in Table 2, compare reasonably well with those of the ground state except for Φ_J, Φ_{KJ} and Φ_K of the $\nu_5+\nu_{10}$ level; this behavior is likely due to the lower J and K_a values reached in the transition assignments of the combination band. The reliability of the parameters obtained was tested by resorting to several spectral simulations in different regions. The comparison between the synthetic and the observed spectra is satisfactory, as indicated by the features depicted in all the figures reported.

Finally, by combining the present value of $\nu_5+\nu_{10}$ with that of the $\nu_5+\nu_{10}-\nu_5$ hot band at 1129.5(2) cm^{-1}, determined from the low-resolution spectra, the ν_5 fundamental is evaluated to occur at 235.9(2) cm^{-1}.

3.3. Fermi Resonance between ν_9 and $\nu_5+\nu_{10}$ Vibrations. As reported in low-resolution studies,[8] the $\nu_5+\nu_{10}$ combination interacts with the ν_9 fundamental through a Fermi resonance. We can extract information on the unperturbed levels and the coupling constant W by using a procedure similar to that of ref 13. A simple 2×2 matrix for the two interacting levels is given by

$$\begin{pmatrix} {E_9}^0 & W \\ W & {E_{510}}^0 \end{pmatrix}$$

where $E_9{}^0$ and $E_{510}{}^0$ represent the unperturbed energies of the interacting levels and W is the perturbation parameter. From diagonalization of this matrix one obtains the perturbed energies E'_9 and E'_{510}:

$$E'_9 = \bar{E} + \frac{1}{2}\sqrt{4W^2 + \delta^2}, \quad E'_{510} = \bar{E} - \frac{1}{2}\sqrt{4W^2 + \delta^2}$$

where

$$\bar{E} = \frac{1}{2}({E_9}^0 + {E_{510}}^0) \qquad \text{and} \qquad \delta = {E_9}^0 - {E_{510}}^0$$

The relative intensities of the two bands depend both on W and on the energy difference between the two unperturbed levels δ and can be evaluated in terms of the eigenvectors of the perturbation matrix. Assuming that the unperturbed $\nu_5+\nu_{10}$ combination has negligible intensity compared to that of unperturbed ν_9 fundamental, the ratio of the band intensities is given by

$$\frac{I_{510}}{I_9} = \frac{\sqrt{4W^2 + \delta^2} - \delta}{\sqrt{4W^2 + \delta^2} + \delta}.$$

Since the two bands are mostly overlapped and their integrated band intensities cannot be compared, the only way to obtain a reliable experimental value of the ratio I_{510}/I_9 is a careful simulation of the resolved fine structure in the spectral regions where transitions arising from the ν_9 and $\nu_5+\nu_{10}$ bands are together present. The best agreement between the synthetic and the observed spectrum is obtained if the $\nu_5+\nu_{10}$ combination is (35 ± 15)% as intense as the ν_9 fundamental. Since we know the perturbed band origins (Table 2), it was straightforward to calculate the unperturbed band origins $E_9{}^0 = 1372.6(8)$ and $E_{510}{}^0 = 1367.9(8)$ cm^{-1} and the Fermi resonance parameter $W = 4.2(5)$ cm^{-1}.

In addition, it should be noted that the resolved structure of the ν_9 and $\nu_5+\nu_{10}$ bands does not reflect irregularities arising from a higher order Fermi perturbation ($\Delta K_a \pm 2$). The calculated reduced rovibrational energies of both levels suggest the presence of several crossings between levels with $\Delta K_a \pm 2$, but the absence of even small deviations near the crossings means that the above interacting effects are very weak and the displacements are of the same order of magnitude or less than the uncertainties of the measurements.

3.4. Ab Initio Anharmonic Force Field Calculation. Electronic energy calculations of ground-state *cis*-difluoroethylene were carried out by means of two electron-correlation procedures. For this molecule the Hartree−Fock determinant strongly dominates the electronic molecular wave function, therefore accurate predictions were given by coupled-cluster theory with single and double excitations augmented by a quasiperturbative term arising from connected triple excitations,[14] CCSD(T).

The other level of theory employed in this investigation was second-order Møller−Plesset many-body perturbation theory,[15,16] MP2.

TABLE 3: Computed and Experimental Geometries of *cis*-1,2-Difluoroethylene: The cc-pVTZ Basis Set Was Used with Both Theoretical Methods

	CCSD(T)	MP2	exptl[a]
*r*CF/Å	1.3369	1.3318	1.339
*r*CC/Å	1.3303	1.3192	1.324
*r*CH/Å	1.0795	1.0701	1.089
∠CCF/deg	122.63	122.77	122.1
∠CCH/deg	122.29	122.07	124.0

[a] r_0 structure from ref 24.

TABLE 4: Computed Anharmonicity Constants x_{ij} (cm^{-1}) of cis-CHF=CHF[a]

i/j	1	2	3	4	5	6	7	8	9	10	11	12
1	−28.08	−3.95	−6.90	−1.69	−0.21	−14.25	−0.82	−112.95	−7.24	−3.24	−0.83	−10.63
2		−6.86	−9.98	−6.04	−1.72	−10.19*	−5.97	45.30	−55.48	−6.89	−5.95	−4.19
3			−1.55	1.13	2.80	−0.16	−1.26	−10.00	−9.37	−7.27	−1.12	1.42
4				−2.23	−2.97	−0.59	−1.46*	−1.78	−4.84	−5.56	−1.82	−0.06
5					0.99	0.94	0.54	0.06	−0.34*	−0.26*	−0.29	0.11
6						−7.60*	−0.59	−10.82	−1.02	−1.46	−0.48	−5.64
7							−0.46*	−0.06	−1.22	−1.61	0.36	−1.99
8								−27.05	35.68	−3.23	−0.44	−10.99
9									−4.96	−4.16*	−2.57	0.43
10										−2.12	−3.14	−1.88
11											−0.24	0.06
12												−0.64

[a] The right upper triangle of the symmetric x_{ij} matrix is given. The constants which are affected by Fermi resonances are marked by asterisk and have the following unperturbed values: $x_{26} = -3.71$, $x_{66} = -9.21$, $x_{47} = 18.37$, $x_{77} = -5.42$, $x_{59} = 0.20$, $x_{510} = -0.80$, $x_{910} = -3.62$.

Since in order to approach chemical accuracy for equilibrium geometry and force field predictions it seems necessary to use spdf-type functions in the basis set for C/F and spd-type functions for hydrogen,[17] all the computations were performed using the atomic-orbital basis set of triple-ζ quality, namely the correlation consistent polarized valence triple-ζ of Dunning,[18] cc-pVTZ, which comprises 148 contracted Gaussian-type orbitals (cGTOs): (5s2p1d)/[3s2p1d] for H atoms and (10s5p2d1f)/[4s3p2d1f] for C and F atoms. The optimized geometry of *cis*-CHF=CHF was calculated at CCSD(T)/cc-pVTZ level theory; the harmonic wavenumbers and the quadratic force fields in a Cartesian representation were then evaluated at the same level of theory.

The expansion of the potential energy for a semirigid polyatomic molecule can be written as

$$\frac{V}{hc} = \frac{1}{2}\sum_{\mathrm{i}}\omega_i {q_i}^2 + \frac{1}{6}\sum_{ijk}\phi_{ijk}q_iq_jq_k + \frac{1}{24}\sum_{ijkl}\phi_{ijkl}q_iq_jq_kq_l$$

where ω_i are the harmonic wavenumbers, q_i the dimensionless normal coordinates, and ϕ_{ijk} and ϕ_{ijkl} the third and fourth order force constants, respectively.

To reduce the computational costs, especially in terms of time, the MP2/cc-pVTZ level of theory was employed to compute the cubic and quartic normal coordinate force constants (ϕ_{ijk},ϕ_{iijk}), which were determined with the use of a finite difference procedure:[19]

$$\frac{\partial^3 V}{\partial q_i \partial q_j \partial q_k} = \phi_{ijk} = \frac{\phi_{jk}(+\delta q_i) - \phi_{jk}(-\delta q_i)}{|2\delta q_i|}$$

$$\frac{\partial^4 V}{\partial q_i \partial q_i \partial q_j \partial q_k} = \phi_{iijk} = \frac{\phi_{jk}(+\delta q_i) + \phi_{jk}(-\delta q_i) - 2\phi_{jk}({q_i}^0)}{|\delta q_i|^2}$$

At the optimized geometry, steps were taken along the normal coordinates and second derivatives of the energy were calculated analytically at each displaced coordinate. These displacements were chosen so that the variation of the potential energy was 0.001 hartree for every vibrational mode. The quantum chemical calculations were carried out with the MOLPRO suite of programs[20] on a SGI Origin 3800 workstation for the CCSD(T)/cc-pVTZ geometry optimization and quadratic force constant calculations. An entirely dedicated PC was employed to compute, using the GAMESS-UK program,[21] the MP2/cc-pVTZ cubic and semi diagonal quartic force constants. Throughout the present investigation, in both levels of theory employed, all electrons were correlated.

The complete third-order force field and the semidiagonal quartic terms suffice, according to second-order perturbation theory,[22] to determine all required molecular spectroscopic properties; effects of Fermi resonances[23] were included by matrix diagonalization.

The computed equilibrium geometries of *cis*-CHF=CHF at the CCSD(T) and MP2 levels of theory are listed in the first and the second column of Table 3, respectively. For comparison, the corresponding experimental bond lengths and bond angles of the r_0 structure determined from microwave spectra,[24] are also shown. There is a general agreement between the calculated and observed structures: the CCSD(T)/cc-pVTZ equilibrium geometry, as expected, reproduces better the experimental one and has therefore been used as reference geometry for the computation of the anharmonic force field, as previously described. The anharmonicity constants x_{ij} of *cis*-difluoroethylene calculated with the theoretical quadratic, cubic, and quartic force fields, are shown in Table 4. The anharmonic interactions between fundamentals and overtones ($\nu_r/2\nu_s$) or combination states ($\nu_r/\nu_s+\nu_t$) may lead to indefinitely large terms in the corresponding perturbational formulas.[22] It is therefore necessary to define effective constants by excluding the respective contributions from the perturbational summations.[22,23] Such effective anharmonicity constants are introduced in the present work to account for the Fermi resonances $\nu_2/2\nu_6$, $\nu_4/2\nu_7$, and $\nu_9/\nu_5+\nu_{10}$; in these cases, the perturbational and variational values for the anharmonic shifts of ν_2 and ν_9 are about 2 cm^{-1} whereas those for ν_4 are up to 7 cm^{-1}.

The Mills and Robiette treatment of the CH stretching vibrations using local modes,[25] can also be applied to this molecule and will give the following $x - K$ relations: $x_{11} = x_{88} = x_{18}/4 = K_{1188}/4$, where K_{1188} is the Darling-Dennison coefficient. The calculated theoretical values are $x_{11} = -28.08$, $x_{88} = -27.05$, $x_{18} = -112.95$, and $K_{1188} = -112.83$ cm^{-1}, in very good agreement with the empirical relations.

The best theoretical estimates of the fundamental vibrational wavenumbers ν_i of *cis*-CHF=CHF are reported in Table 5 together with the harmonic wavenumbers computed at the two levels of theory employed in the present investigation. The theoretical harmonic wavenumber ω_i in the first column of Table 5 were obtained from MP2/cc-pVTZ calculation together with the intensity, reported in the second column of the same table. In the third column, the harmonic wavenumbers were obtained from CCSD(T)/cc-pVTZ theory, and in the last column of the same table, the fundamental wavenumbers ν_i were computed applying the x_{ij} anharmonicity constants of Table 4; the values in parentheses correspond to explicit treatment of the cubic interactions.

TABLE 5: Calculated Harmonic (ω_i/cm^{-1}) and Fundamental (ν_i/cm^{-1}) Vibrational Wavenumbers for *cis*-CHF═CHF, along with the Infrared Intensities (A_i/km mol^{-1}): Both Theoretical Methods Employed the cc-pVTZ Basis Set

	MP2		CCSD(T)	
i	ω_i	A_i	ω_i	ν_i
1	3311	5.4	3255	3118
2	1801	52.7	1765	1720 (1722)[a]
3	1308	33.6	1292	1269
4	1039	58.3	1026	1009 (1016)[a]
5	233	2.2	234	235
6	900	-	843	807
7	528	-	506	498
8	3280	5.4	3231	3142
9	1432	32.2	1413	1379 (1380)[a]
10	1174	113.5	1162	1139
11	787	28.7	776	768
12	810	44.3	778	761

[a] Value coming from the diagonalization of the interaction matrix.

The treatment of Fermi interactions was performed by diagonalizing the matrix formed by the unperturbed calculated ν_i and the resonance term $W = \phi_{rst}/\sqrt{8}$, where ϕ_{rst} is the cubic force constant in dimensionless coordinates space. For the ν_9/$\nu_5+\nu_{10}$ dyad, $\phi_{9,510}$= 8.59 cm^{-1} and therefore $W = 3.04$ cm^{-1}, which is in agreement with the 4.2(5) cm^{-1} value of section 3.3.

Considering that no scaling factors nor fits to experimental data were introduced, there is a general good agreement between the observed wavenumbers (Table 1) and the computed ν_i. The largest discrepancy is in ν_6, an infrared inactive band.

4. Conclusions

This work reports a high-resolution infrared study of *cis*-CHF═CHF in the region 1350−1391 cm^{-1} of atmospheric interest. Many transitions belonging to the ν_9 fundamental and the $\nu_5+\nu_{10}$ combination band have been identified and the measurements have yielded sufficient information to obtain accurate spectroscopic parameters for the excited states. Several spectral simulations in different regions were used to test the reliability of the constants obtained and to determine the relative intensities of the two bands analyzed. A Fermi resonance treatment of the perturbed ν_9 and $\nu_5+\nu_{10}$ levels led to estimates of the coupling constant and the unperturbed band origins for the two vibrations. Correlated harmonic CCSD(T)/cc-pVTZ and anharmonic MP2/cc-pVTZ force fields provided theoretical predictions for the fundamental wavenumbers and the perturbing levels. *Cis*-CHF═CHF belongs to halogenated ethylenes involved in atmospheric chemical processes and studies for simulations of the absorptions of this trace gas in the atmospheric window have to rely to high-resolution infrared analysis, which has previously not been available.

Acknowledgment. The authors thank A. Baldan for the synthesis of the sample. Financial support by MIUR, Rome, is gratefully acknowledged.

Supporting Information Available: Complete list of the assigned transitions of the ν_9 (Table 1S) and $\nu_5+\nu_{10}$ (Table 2S) bands of *cis*-1,2-difluoroethylene; cubic normal (Table 3S) and quartic normal (Table 4S) coordinates force constants; definition of internal and symmetry coordinates, quadratic symmetric force constants, and eigenvectors, which define the normal coordinates of *cis*-1,2-difluoroethylene (Table 5S). This material is available free of charge via Internet at http://pubs.acs.org.

References and Notes

(1) Atkinson, R.; Aschmann, S. M.; Goodman, M. A. *Int. J. Chem. Kinet.* **1987**, *19*, 229.

(2) Atkinson, R. *Atmos. Environ.* **1990**, *24A*, 1.

(3) Stoppa, P.; Giorgianni S.; Gambi A.; De Lorenzi, A.; Ghersetti, S. *Mol. Phys.* **1995**, *84*, 281.

(4) Visinoni, R.; Giorgianni, S.; Baldacci, A.; Ghersetti, S. *J. Mol. Spectrosc.* **1998**, *190*, 248.

(5) Stoppa, P.; Giorgianni, S.; Ghersetti, S. *Mol. Phys.* **1996**, *88*, 533.

(6) Visinoni, R.; Giorgianni, S.; Stoppa, P.; Ghersetti, S. *Spectrochim. Acta Part A* **2000**, *56*, 1887.

(7) Visinoni, R.; Giorgianni, S.; Baldan, A.; Nivellini, G. *Phys. Chem. Chem. Phys.* **2001**, *3*, 4242.

(8) Craig, N. C.; Overend, J. *J. Chem. Phys.* **1969**, *51*, 1127.

(9) Bock, C. W.; George, P.; Trachtman, M. *J. Mol. Spectrosc.* **1979**, *76*, 191.

(10) Kagel, R. O.; Powell, D. L.; Overend, J.; Ramos, M. N.; Bassi, A. B. M. S.; Bruns, R. E. *J. Chem. Phys.* **1983**, *78*, 7029.

(11) Laurie, V. W. *J. Chem. Phys.* **1961**, *34*, 291.

(12) Guelachvili, G.; Narahari Rao, K. *Handbook of Infrared Standards*; Academic Press: London, 1986.

(13) Escribano, R.; Domenech, J. L.; Cancio, P.; Ortigoso, J.; Santos, J.; Bermejo, D. *J. Chem. Phys.* **1994**, *101*, 937.

(14) Raghavachari, K.; Trucks, G. W.; Pople J. A.; Head-Gordon, M. *Chem. Phys. Lett.* **1989**, *156*, 479.

(15) Møller, C.; Plesset, M. S. *Phys. Rev.* **1934**, *46*, 618.

(16) Hampel, C.; Peterson, K.; Werner, H.-J. *Chem. Phys. Lett.* **1992**, *190*, 1.

(17) Császár, A. G. Anharmonic Molecular Force Fields. In *The Encyclopedia of Computational Chemistry*; Schleyer, P. V., Allinger, N. L., Clark, T., Gasteiger, J., Kollman, P. A., Schaefer, H. F; III; Schreiner, P. R., Eds.; John Wiley Sons: Chichester, 1998.

(18) Dunning, T. H., Jr. *J. Chem. Phys.* **1989**, *90*, 1007.

(19) Schneider, W.; Thiel, W. *Chem. Phys. Lett.* **1989**, *157*, 367.

(20) MOLPRO is a package of ab initio programs written by Werner, H.-J.; Knowles, P. J. with contributions from Amos, R. D.; Bernhardsson, A.; Celani, P.; Cooper, D. L.; Deegan, M. J. O.; Dobbyn, A. J.; Eckert, F.; Hampel, C.; Hetzer, G.; Korona, T.; Lindh, R.; Lloyd, A. W.; McNicholas, S. J.; Manby, F. R.; Meyer, W.; Mura, M. E.; Nicklass, A.; Palmieri, P.; Pitzer, R.; Rauhut, G.; Schütz, M.; Stoll, H.; Stone, A. J.; Tarroni R.; Thorsteinsson, T.

(21) GAMESS-UK is a package of ab initio programs written by Guest, M. F.; van Lenthe, J. H.; Kendrick, J.; Schoffel, K.; Sherwood, P. with contributions from Amos, R. D.; Buenker, R. J.; van Dam, H. J. J.; Dupuis, M.; Handy, N. C.; Hillier, I. H.; Knowles, P. J.; Bonacic-Koutecky, V.; von Niessen, W.; Harrison, R. J.; Rendell, A. P.; Saunders: V. R.; Stone, A. J.; Tozer, D. J.; de Vries, A. H.. The package is derived from the original GAMESS code due to Dupuis, M.; Spangler, D.; Wendoloski, J. NRCC Software Catalog, Vol. 1, Program No. QG01; Daresbury Laboratory, UK, 1980.

(22) Mills, I. M. *Molecular Spectroscopy: Modern Research*; Narahari Rao, K., Mathews, C. W., Eds.; Academic Press: New York, 1972; Vol. 1, pp 115−140.

(23) Papoušek, D.; Aliev, M. R. *Molecular Vibrational−Rotational Spectra*; Elsevier: Amsterdam, 1982.

(24) Laurie, V. W.; Pence, D. T. *J. Chem. Phys.* **1963**, *38*, 2693.

(25) Mills, I. M.; Robiette, A. G. *Mol. Phys.* **1985**, *56*, 743.